JOURNAL OF GEOPHYSICAL RESEARCH, VOL. 102, NO. A7, PAGES 14,189–14,198, JULY 1, 1997

Super storms

J. T. Bell, M. S. Gussenhoven, and E. G. Mullen
Phillips Laboratory, Hanscom Air Force Base, Massachusetts

Abstract. "Super storms" are defined to be the largest 2% of geomagnetic storms from 1932 through 1995, selected using ground-based magnetic indices. These storms are significant not only because they are prolonged periods of extremely high magnetic activity but also because data taken during super storms in the space era show other anomalous features, such as abnormally high energy input to the auroral regions from precipitating particles, and/or the creation of additional, trapped radiation belts in the inner magnetosphere. Super storms are most likely to occur on the downslope from solar maximum and near the equinoxes. One half of the super storms have multiple SSCs that reactivate magnetospheric currents and prolong magnetic activity. *AE* "spikes" occur during some of the super storms. The relationship between super storms and the locations of trapped radiation populations is briefly examined. The auroral energy input to the inner magnetosphere during recent super storms is calculated and presented.

1. Introduction

Since the start of the space program in the 1960s, measurements within the magnetosphere have revealed the profound influence of extremely large magnetic storms on space plasma and particle populations. Two of the most documented storms occurred in August 1972 (see *Spjeldvik and Fritz* [1981a] for a list of references) and March 1991 [*Blake et al.*, 1992b; *Daly et al.*, 1992; *Fredrickson et al.*, 1992; *Gussenhoven et al.*, 1992; *Mullen et al.*, 1991; *Mullen and Gussenhoven*, 1994; *Mullen and Ray*, 1994; *Shea et al.*, 1992; *Violet and Fredrickson*, 1992]. These major magnetic storms, which we call super storms, are of great interest to the scientific community for two main reasons: (1) they drive the magnetosphere to an extreme state where dynamic processes, obscure under lesser conditions, can be clearly identified and studied; and (2) they create extremely enhanced electromagnetic fields and particle environments that behave differently than predicted by conventional theory.

The March 1991 storm is a case in point. A significant factor in making the magnetospheric environment so harsh during the March storm was the creation of new stably trapped energetic electron and proton belts in the slot region (at L values between 2 and 3 R_E) at the beginning of the storm period [*Mullen et al.*, 1991; *Blake et al.*, 1992a, b]. The Combined Release and Radiation Effects Satellite (CRRES) was well positioned and instrumented to measure the formation of the new belts in response to the passage of a strong solar wind shock(s). Data from CRRES led to new efforts in modeling the acceleration of particles by induced electric fields and revealed how effectively particles can be energized when they drift in resonance with the electric field pulse [*Li et al.*, 1993; *Hudson et al.*, 1995; *Ginet et al.*, 1994].

Although in situ space measurements are only available for parts of the last three solar cycles, ground-based observations of the Earth's magnetic field have been recorded for over a century [*Legrand and Simon*, 1981; *Feynman*, 1983]. These observations have been used to produce various magnetic indices. Two of the indices, *Kp* (logarithmic) and *ap* (linear), are planetary magnetic indices that are available from 1932 to the present. Calculation of the ring current index (Dst) and the auroral electrojet index (AE), began with the space age in 1957 [*Mayaud*, 1980]. These magnetic indices (particularly *Kp* and Dst) have traditionally been used to identify geomagnetic storms [*Joselyn and Tsurutani*, 1990]. Methods of identifying geomagnetic storms have ranged from the qualitative ("It's obviously a storm.") to the quantitative ($Dst \leq -100$ nT). Even though quantitative criteria can be (by and large) arbitrary, they have been found to be useful. Magnetic indices have also been used to characterize "larger" and "largest" storms.

The purpose of this paper is to identify the top 2% of magnetic storms since 1932 (our "super storms"), using the available *ap*, *Kp*, Dst, and AE data. We examine these storms in some detail, focusing on when they occur, similarities in their morphology, long-term changes to trapped particle populations, and auroral energy input levels.

2. Selection of Storms

The magnetic indices we used in this study cover the period from 1932 through 1995. Quantitative selection criteria were developed for four magnetic indices (*Kp*, *ap*, Dst, and AE) and used to select the largest storms for each index. The process that led to these criteria was evolutionary in nature, with the criteria and values used being adjusted slightly at each step. Combinations of various criteria were used to assure that the super storms had both large magnitudes and long durations.

Initially, we considered using only the magnitude of magnetic activity to select the largest storms. However, for the small number of storms we wished to select this proved impractical, particularly for *Kp* and *ap* (too many storms contain the maximum possible values for *Kp* and *ap*). It also resulted in the occasional selection of brief, but very intense periods of magnetic disturbance, periods that did not affect the particle populations as strongly as longer lasting storms. Therefore the largest storms for each index were selected by requiring a combination of disturbance magnitude and duration of the disturbance. After the largest storms for each index were selected the results were compared. Some storms were selected

Paper number 96JA03759.

as largest by more than one index, while others were not. The super storms were expected to enhance all of the magnetic indices, although not necessarily to the point where they would be selected as largest using all four indices. The storms that had the greatest effect on the largest number of indices, were selected as super storms. Although the precise values used to select them are somewhat arbitrary, a brief examination of the data leaves no doubt that the super storms include the largest geomagnetic storms since 1932.

2.1. Database

The four indices used in this study are briefly described below. *Mayaud* [1980] provides more detailed information. The data were downloaded from the National Geophysical Data Center (NGDC) in Boulder, Colorado (except for the preliminary values of AE) at ftp.ngdc.noaa.gov/STP/GEOMAGNETIC_DATA/INDICES/.

The Kp and ap indices are different representations of the same data set. Kp is based on the peak magnetic activity recorded by a network of ground magnetometer stations. There are 28 possible values ranging from 0 to 9 in thirds (0, 0+, 1−, 1o, 1+, 2−, ···,), for each 3-hour period. These values scale approximately logarithmically with planetary magnetic activity. The ap index is a linear version of Kp, with a linear scale from 0 to 400, but still with only 28 possible values. The ap index was originally developed to provide a statistically correct method of working with average values of Kp (it is not statistically correct to average values on a logarithmic scale). We wished to use Kp because it is a widely used index, but we also wished to work with time averaged values when selecting storms. So we used storm selection criteria that involved time averaging for ap but developed other criteria for Kp. Both indices are included in this study, because the different criteria produced different results. Data from January 1932 through February 1996 are available for both indices.

The Dst index provides a measure of the strength of the equatorial ring current, relative to quiet conditions. It is produced using magnetic data from a series of low-latitude observatories. It has a time resolution of 1 hour, is measured in nanotesla, and becomes negative during geomagnetic storms. The Dst index is available from January 1957 through December 1995.

AE is the auroral electrojet index. It is an hourly value based on a network of high-latitude observatories and provides a measure of the strength of the auroral electrojet. The AE index is available from July 1957 through June 1988, with a 2-year gap in 1976 and 1977. We also have access to preliminary AE values for March 1989 and December 1990 through March 1991. The preliminary values are used to examine the morphology of the super storms, but not to select the super storms.

2.2. Individual Index Storm Selection Criteria

Magnetic storms are commonly identified as time periods of large deviations from background levels in ground-based magnetometer data. Some of the more common storm definitions require $Dst \leq -100$ nT or $Kp \geq 6o$. This is equivalent to $ap \geq 80$ or roughly $AE \geq 600$ nT. Each of these criteria identify magnetic storms, but the resulting storms are not necessarily the largest or the ones that have the most impact on the state of the inner magnetosphere. We have only found four documented periods in the literature [*Gussenhoven et al.*, 1989; *McIlwain*, 1963; *Mullen et al.*, 1991; *Spjeldvik and Fritz*, 1981b] with evidence for the formation of significant trapped high-energy particle populations in the "slot region" between 1960 and 1995. For Dst, using the −100-nT level as the selection criteria, there are approximately 324 magnetic storms. If four of these storms coincided with new trapped particle populations, that would be 1.3% of the storms. However, some additional periods with trapped particles may have been missed, because continuous space particle measurements are not available. Between 1983 and 1992, a period of 10 years for which DMSP and CRRES provide good particle coverage, we saw two major long-lasting, high-energy, trapped particle populations in the slot region. This is about 1.5 times as many as expected based on the 1.3% criteria. We therefore chose to select the largest 2% of all storms as "super storms." We identified the 7 largest storms in the 3.5 solar cycles over which Dst is available, or on average about 2 per solar cycle. We apply this rate to the other indices as well and attempt to select an average of 2 largest storms per solar cycle using each index. A further selection, taking into account all the indices then is made. The selection process is explained in detail below.

2.2.1. *Kp* selections. We select the 13 largest storms from the 64 years of Kp data to meet the 2% criterion. The selection criteria using Kp were the most difficult to develop. It is inappropriate to use average values of Kp because it has a logarithmic scale. We experimented with using peak disturbances, requiring a specified disturbance for some length of time, and allowing brief periods of lower disturbance during the storm. We finally combined these methods and used the following criteria for selecting large storms using Kp: Kp had to be above a threshold ($T1$) for a specified number of readings (A) out of a larger number of consecutive readings (B) and at least one of the readings had to be above a second higher threshold ($T2$). $T1$ and $T2$ control the magnitude of the selected storms. A and B specify the required duration, allowing for brief periods of relaxation (which are common in the larger storms). The final parameters for selection of the largest storms, were reached by a repeated process of setting the parameters and then qualitatively comparing the selected storms with nonselected storms. The final selection criteria were Kp must be greater than or equal to 6o for 14 of 19 consecutive readings and at least one value must be greater than or equal to 9−. These criteria selected the 13 storms listed in Table 2. If we had simply picked periods for which Kp exceeded 9− we would have selected four times as many storms. The storms chosen by our criteria maintain very high levels of magnetic activity for about 2 days.

2.2.2. The *ap* selections. For ap we also selected the 13 largest storms. We initially used the following criteria to select the largest storms: the average value of ap over a specified number of readings (A) had to be greater than or equal to a threshold value (T), where A specifies the minimum duration and T the minimum magnitude of the storms to be selected. However, there were many settings for A and T that led to selection of 13 storms. To assure that the "largest" storms had both high magnitude and long durations, we compared the selection results from nine different combinations of A and T (with A ranging from 1/2 to 4 1/2 days in 1/2-day increments). The most frequently selected storms for each combination of A and T as shown in Table 1 were considered the largest and are indicated by an asterisk in the table. Thirteen storms met the criteria for over half the A,T combinations. We note that the average ap over a 2-day interval is at least 142 (corresponding to $Kp > 7o$) for all but 1 of the storms selected as largest.

Table 1. "Largest" Storms, Selected Using *ap*

Storm Start (Approximate)		Threshold Value (Duration Required)†								
Year	Day	90 (4½ day)	98 (4 day)	108 (3½ day)	118 (3 day)	124 (2½ day)	142 (2 day)	172 (1½ day)	220 (1 day)	285 (½ day)
1940*	84	X	X	X	X	X	X	X	X	X
1940*	89	X	X	X	X	X	X	X	X	
1941	60									X
1941	186								X	X
1941*	261	X	X	X	X	X	X	X	X	X
1946	82	X	X	X	X					
1946	207									X
1946*	265			X	X	X	X	X		
1957	247	X	X	X					X	
1957	264				X					
1958	42									X
1958	189							X		X
1959	85	X	X	X	X					
1959*	196	X	X	X				X	X	X
1960*	91	X	X	X	X	X	X	X	X	
1960*	280	X	X	X	X	X	X	X	X	X
1960*	317	X	X	X	X	X	X	X	X	X
1967	145							X	X	X
1972*	217	X	X	X	X	X	X	X	X	
1982*	194	X			X	X	X	X	X	X
1982	248					X	X			
1986*	39		X	X	X	X	X	X	X	X
1989*	72	X	X	X	X	X	X	X	X	X
1991*	83	X	X	X	X	X	X			
1991	155						X			

*Super storms selected using *ap*.
†All threshold values are averages.

2.2.3. *Dst* selections. We selected seven largest storms from the *Dst* indices to meet the 2% criterion. A procedure similar to that used for *ap* was used for *Dst*. Here A again specified the minimum duration, but the threshold value T was a maximum allowable level rather than a minimum due to the negative values of *Dst*. Again, nine different combinations of A and T were used with A having the same ranges as for *ap*. A table similar to Table 1 was prepared, but for brevity it is not shown here. The seven storms selected satisfied six or more of the nine A, T combinations. The storms are listed in Table 2.

2.2.4. *AE* selections. For the AE indices we again selected seven largest storms. The methods used for *ap* and *Dst* were applied to AE with somewhat disappointing results. While *ap* and *Dst* had several storms that were selected for all durations, AE did not. In fact, there were no storms selected by eight or nine of the A,T combinations. A total of 23 storms were selected at least once with 7 meeting the criteria for half (5 or more) the A,T combinations. These seven storms were taken to be the "largest" storms according to AE. The storms selected using AE were generally much more sensitive to the criteria used than the storms for *ap* or *Dst*. In general, the AE storms appeared to have either long durations of moderate disturbance or short times of very intense disturbance. The provisional AE values that were prepared for the March storms in 1989 and 1991 were not included in these selections. If they had been considered, using the duration-threshold conditions described above, both storms would have been selected.

Table 2. Super Storms by Index

Storm		Index			
Year	Day	*Kp*	*ap*	*Dst*	AE
1940*	84	X	X		
1940*	89	X	X		
1941	261		X		
1946	82	X			
1946*	265	X	X		
1957*	247	X		X	
1957	264	X			
1959*	196		X	X	
1960*	91	X	X	X	
1960	118				X
1960	197				X
1960*	280	X	X		X
1960*	317		X	X	
1965	166				X
1967	145			X	
1972*	217	X	X		
1978	120				X
1982*	194		X		X
1982	248	X			
1986*	39	X	X		X
1989*	72	X	X	X	P
1991*	83	X	X	X	P

*Super storms. X, selected; P, provisional AE values.

2.3. Super Storm Selections

Table 2 is a composite of the "largest" storms selected using each index. There are a total of 22 storms that are selected using at least one index. For the 1989 and 1991 storms, P in the AE column indicates that provisional AE values would select the storms as largest storms. The only storms that are selected by all four magnetic indices are these two storms, when we use the provisional AE values. In the period from 1957 to 1986, when all indices were available (without provision) no storm is selected by all four indices. Three are selected by three indices,

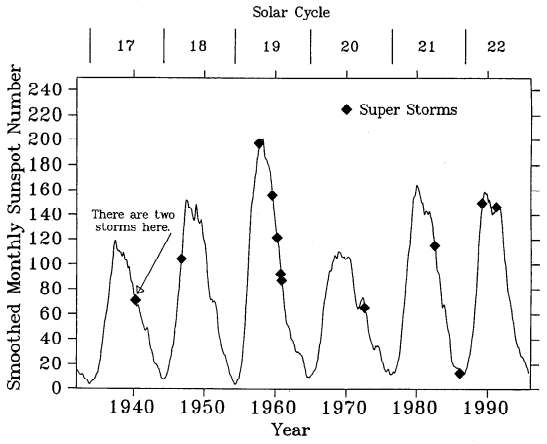

Figure 1. Solar cycle and super storm occurrence.

and five are selected by two. In the period prior to 1957, when no *Dst* or *AE* indices existed, three storms are selected by both *Kp* and *ap*. We designate the 13 storms that are selected as largest storms by at least two indices, as super storms.

It initially appeared that the lack of additional indices from 1932 through 1956 might have resulted in a significantly lower number of super storms during that time. However, comparison of the distribution of super storms with the distribution of largest storms selected using *Kp* and *ap* indicate that this is not the case. Three of the super storms or 23% occur prior to 1957. There are five largest storms prior to 57, when only *Kp* and *ap* are available. This is 29% of all the storms selected as largest using only *Kp* and *ap*. The difference between these two percentages is less than one super storm (7.7%).

If one wished to use a single index to select the largest storms, *AE* would be a poor choice. It produces the most distinctive results of the four indices used and has the least impact on which storms are selected as super storms. Except for the 1989 and 1991 storms, using the provisional *AE* values, the storms selected using *AE* do not overlap with those selected using *Dst*. Four of the storms selected as largest using *AE* are not selected using any of the other indices. In fact, if *AE* were not used at all, only one super storm would be lost.

At the opposite extreme *ap* is very useful for selecting eventual super storms. Of the 13 storms selected using *ap*, all but one (that occurring in 1941) are selected to be super storms, and *ap* only misses one super storm (that in 1957).

2.4. Super Storm Occurrence

It is important to know where in the solar cycle super storms occur, to see if any obvious solar cycle dependence exists. Figure 1 is a plot of the smoothed monthly sunspot numbers from 1932 through 1995, with super storms indicated by solid diamonds. In 1940, two of the super storms are so close together that only one diamond is visible. This plot includes almost six complete solar cycles, which are identified above the plot.

Figure 1 shows that most of the super storms (nine) occurred on the downslope from solar maximum. Two occurred nearly at solar maximum, one occurred during solar minimum, and one occurred when sunspot numbers were increasing. Of the 13 super storms, only two occurred when the monthly smoothed sunspot numbers were below the median value (65.7) for the period from 1932 through 1995. These two were in 1972 and 1986. We see that super storms can occur anywhere in the solar cycle, but the highest probability is on the downslope from solar maximum.

One other noteworthy feature of Figure 1 is the concentration of super storms (five) during solar cycle 19. Cycle 19 had the highest sunspot numbers with the peak exceeding 200. The other solar cycles each have only one or two super storms. This is similar to the results shown by *Cliver and Crooker* [1993] for great storms. A claim might be made that solar cycles with very large peaks (sunspots >200) will have many more super storms, but more data are needed to verify it. Most solar cycles, however, appear to have only one or two super storms.

It has been known for some time that magnetic activity and the number of large magnetic storms increase near the equinoxes relative to the solstices [*Cliver and Crooker*, 1993; *Crooker et al.*, 1992; *Russell and McPherron*, 1973). We decided to see if the same pattern held for super storms. Figure 2 shows the distribution of super storms versus time of year. The year was divided into eight equal segments with four periods centered at the equinoxes and solstices and four periods in between. The number of super storms in each eighth of a year was counted and plotted in histogram format. Eight of the 13 super storms occur near the equinoxes. Five of these storms were near the spring equinox. None of the super storms occurred near the winter solstice, but two were near the summer solstice. This suggests that super storms, like lesser magnetic storms, are more likely to occur near the equinoxes but are not limited to these times only.

3. Morphology of Super Storms

We have found that many of the super storms have common features and occur under similar geophysical conditions which we discuss below. Multiple storm sudden commencements (SSCs) occur during more than half of the super storms, suggesting that multiple shocks in the solar wind pass the earth during these storms. The magnetic indices respond similarly following each SSC. The profiles of magnetic indices for some of the remaining super storms match the behavior of the indices following the SSCs, suggesting that the magnetosphere is subject to multiple shock passages during these storms also. This raises the question of the significance of shock passages in the formation of super storms. Unfortunately, there is insufficient data to answer this question. We know that the SSC list

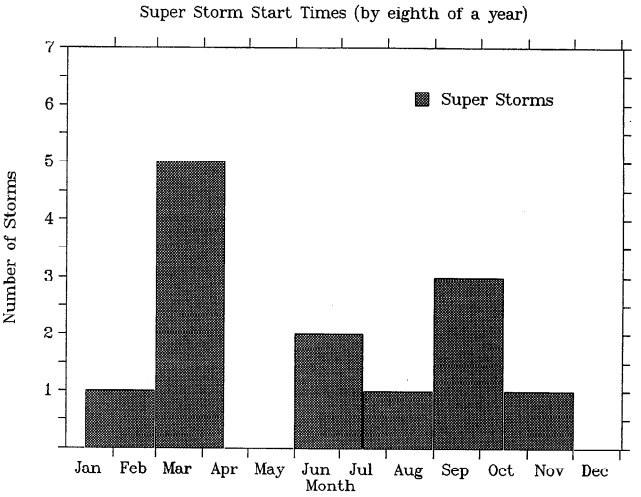

Figure 2. Super storms versus time of year.

does not identify all shocks. We will illustrate this using the one super storm for which there is relatively complete solar wind data. Large AE spikes were recorded during some of the super storms. These occur rarely in the AE database but occur during four of the super storms, for which AE is available.

3.1. Organizing Super Storms by Storm Sudden Commencements

The storm sudden commencement lists used for this work are available on-line at NGDC. The NGDC lists are is based on Mayaud's SSC lists for 1868–1982, and the Preliminary Reports of the International Service of Geomagnetic Indices for 1982 to present. They are available at ftp.ngdc.noaa.gov/SOLAR_DATA/SUDDEN_COMMENCEMENTS/. The portion from 1982 to the present is based on the Preliminary Reports of the ISGI. The lists do not contain a clear specification of the magnitude or strength of the SSCs. They are primarily a compilation of the SSCs reported by various magnetic observatories. We considered that the strength of SSCs might play a role in determining storm behavior and therefore assigned each SSC a number, from 1 to 6, representing the relative size or strength of the SSC, 6 being the strongest. This number was based on the number of stations reporting an SSC and the size of the SSC they reported. It is, by its nature, imprecise, but serves as an indicator of relative SSC size. All SSCs in a 10-day period centered on each super storm were examined.

Of the 13 super storms, 7 storms had two or more strong SSCs, one at the onset of magnetic activity, and a second occurring 4 hours to 3 days later; 3 storms had single SSCs that occurred at the onset of the magnetic activity and were followed by a single deep Dst minimum; and 3 storms could not be well-classified by their SSCs.

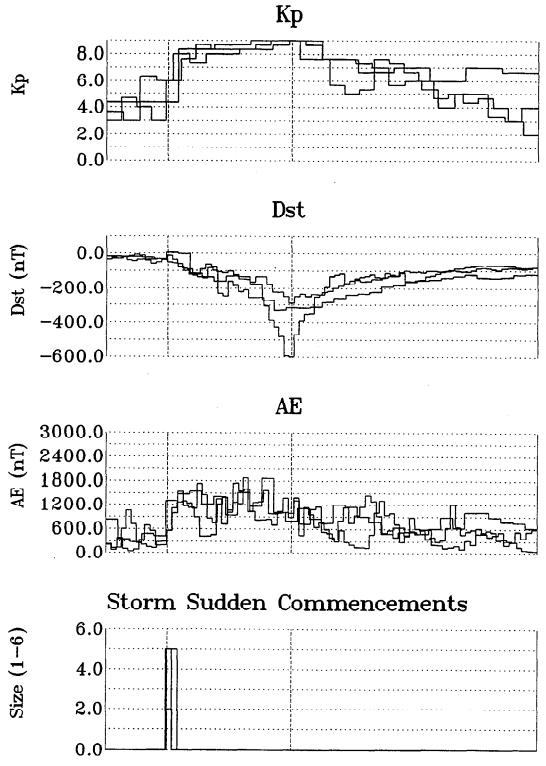

Figure 3. Overlay of super storms from October 1960, August 1982, and March 1989.

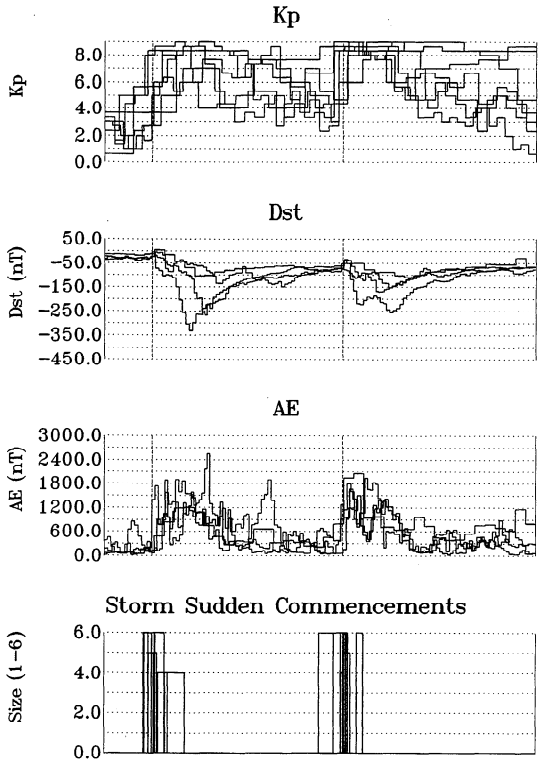

Figure 4. Overlay of storms from March 1940, April 1940, September 1946, September 1957, July 1959, November 1960, and August 1972.

We performed separate analyses for the three storms with single SSCs and the seven storms with multiple SSCs. For the first set of storms we examined the storm evolution in the indices by normalizing the times between SSC onset and Dst minimum and overplotting the indices. For the second set we examined the multiple storm evolutions in the indices by normalizing the times between successive SSC commencements and overplotting the indices. Figures 3 and 4 show the results of these analyses, overlaying the Kp profiles in the top panel, the Dst profiles in the second panel, the AE index profiles in the third panel, and the SSC(s), as bars, in the bottom panel. The vertical dashed lines indicate the two points of normalization for each storm.

The three super storms characterized by a single SSC in Figure 3 occurred in October 1960, August 1982, and March 1989. All follow the classic textbook model of a geomagnetic storm, but with extremely high values of magnetic indices. Each storm closely follows an SSC, which is presumably related to the passage of a shock in the solar wind. Within an hour of the SSC, Dst increases by 10–50 nT, there is an abrupt increase in Kp and AE levels increase sharply. Within 2–3 hours, Dst begins to fall. Kp and AE remain large until Dst reaches a deep minima and begins to recover. Then Kp and AE begin to decrease. The time between the SSC and the Dst minimum ranges from 12 to 24 hours. In each of these three storms, Kp reaches the maximum value of 9, Dst falls below -290 nT, and AE exceeds 1500 nT.

The seven super storms with multiple SSCs (March 1940, April 1940, September 1946, September 1957, July 1959, November 1960, and August 1972) are shown in Figure 4. They appear as "double storms," when they are ordered by the first two SSCs. The double storm nature is not so apparent when

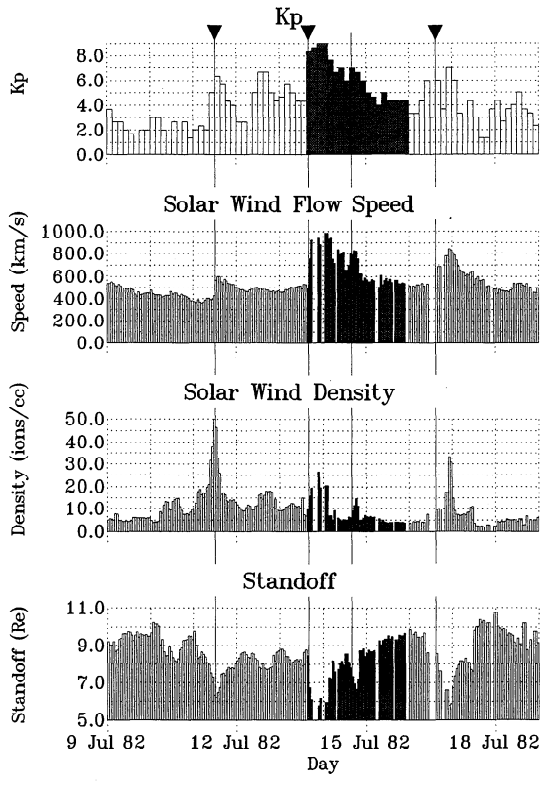

Figure 5. Solar wind data for super storm in July 1982.

actual timescales are used, since the time between SSCs is highly variable. Both SSCs in the double storms precede behavior similar to that observed for the single storms in Figure 3. They each coincide with a positive jump in *Dst* and precede increases in *Kp* and *AE*. In all these cases, *Dst* reaches a local minima between the SSCs, in some cases it drops lower after the second SSC. The extreme values of the magnetic indices for the storms are very large in almost all cases (*Dst* for the August 1972 storm is a notable exception since *Dst* did not fall below −150 nT). One of the storms (November 1960) exhibits a spike in *AE* that exceeds 2400 nT. This occurs as *Dst* recovers after the first SSC, but before the second SSC.

The remaining three super storms do not follow either of the patterns described above, but if we were able to use the passage of shocks in the solar wind, instead of SSCs, it might be possible to include them. For the following discussion it is helpful to bear in mind that the typical response of the magnetosphere to the passage of a shock in the solar wind is an abrupt increase in the magnetic activity. Whether this increased activity level is sustained or not depends on several factors, such as the prior condition of the magnetosphere and the behavior of the solar wind behind the shock front. The first of the three super storms, the one in March/April 1960, does not begin with an SSC. Large disturbance levels were reached, but no SSCs were recorded, until near the end of the storm. However, this storm might follow a shock passage, since there are several points at which the magnetic indices respond in the manner typically associated with shock passages. The storm in February 1986 has an SSC associated with it, but the SSC occurs almost a day prior to when we see the storm onset. The behavior of the magnetic indices at storm onset however, strongly suggests the passage of a shock, shortly before onset. The third storm, in March 1991, has a clear double peak, indicative of two shocks, but there is only a single SSC recorded even though satellite data show the presence of a second shock at the Earth in the middle of this storm. The March 1991 storm appears to belong in Figure 4, but no second SSC was reported.

3.2. Solar Wind Shocks: A Need to Know

The last three cases point out a major gap in our understanding of the causes of super storms. We believe the passage of shocks in the solar wind to be a significant factor in the development of super storms. However, it is not clear what the role of these shocks truly is. We are also interested in these shocks, because of their apparent impact on the trapped particle populations (see Effects on Trapped Radiation Populations). Unfortunately, there is no consistently reliable indicator for identifying shocks in the solar wind or the extent of their effects on the Earth's magnetosphere for the time frame covered by this study. Part of the problem is the lack of adequate satellite databases with solar wind shock information, and part is the weak link between the current SSC databases and the passage of shocks in the solar wind. SSCs do not always correspond to shocks [*Joselyn and Tsurutani*, 1990], and available data show that shocks are not always recorded as SSCs. This is especially the case if a shock hits the magnetosphere during an ongoing geomagnetic substorm, when the effects of the shock on ground-based magnetometers can be masked by the effects of the substorm. Even when shocks are measured as SSCs, there is no information on the strength of the shock. Thus we have no way of consistently identifying shock passages and determining their relationship to super storms.

When solar wind data are available, they provide the desired information on shocks. Unfortunately solar wind data are usually not available during the super storms. Many of the super storms occurred before space data were available. All of the others, with the exception of the storm in July 1982, either occurred during or caused gaps in the solar wind data set. The data from July 1982 does contain a few gaps, but it is still reasonably complete. Figure 5 shows magnetic index and solar wind data for a 10-day period around the July 1982 super storm (shaded region). *Kp* values are in the top panel, the solar wind flow speed and density are in the middle panels, and the standoff distance of the magnetopause calculated by balancing the magnetic and kinetic pressures is in the bottom panel. (The solar wind data is from the OMNI data set at the National Space Science Data Center A.) Triangles mark the SSCs from the NGDC database, and vertical lines indicate shocks which caused the stand-off distance to move sharply inside of 7 R_E. Data gaps immediately after the storm onset may have resulted in incomplete shock data even for this case.

There were three SSCs reported during the 10-day period shown in Figure 5. We can also identify four shocks that drive the magnetopause to near or below geosynchronous altitudes from sharp increases in the solar wind speed and density. The first SSC on July 11 is near a shock that lowers the stand-off distance to 6.3 R_E, and it initiates a small magnetic storm. The second SSC on July 13 initiates the super storm. There may be up to three shocks near the time of this SSC (hidden by data gaps) driving the magnetopause to 6.1, 5.7, and 5.9 R_E, respectively. No SSC is identified on July 14, but the standoff distance, having relaxed out to 8.5 R_E after the compression(s) on July 13 is driven in to 6.7 R_E during the second half of the day. Finally, the SSC, occurring late on July 16 is associated with a strong shock that compresses the magnetopause to 5.8 R_E. The

number of strong shocks clearly indicates an extended period of enhanced solar activity. This super storm follows a period of increased magnetic activity, which may affect the response of the magnetosphere to the shock passage on July 13. We can speculate that super storms require solar wind shocks with following kinetic pressures high enough to push the magnetopause inside L values of 6 R_E, but we cannot adequately test this hypothesis without continuous, high-quality solar wind data.

3.3. *AE* Spikes

While analyzing the AE data for the super storms, a unique feature (a "spike" in the hourly AE values) was observed during four of the storms (November 1960, August 1972, February 1986, and March 1991). These spikes are characterized by the hourly value of AE exceeding 2000 nT, for one or two hours. The AE values the hours before and after the spikes are at least 500 nT lower. There are eight times, in the regular data set that AE exceeds 2000 nT and once in the preliminary data (Table 3). Two of these values are consecutive (in November 1960), so there are a total of eight recorded AE spikes. Of these spikes, four occur during super storms, two closely follow SSCs. One of the reasons we comment on the AE spikes is that evidence exists for the creation of new, long-lasting, high-energy, trapped radiation populations during all four of these super storms.

4. Effects on Trapped Radiation Populations

In this section we will briefly examine measurements of trapped radiation populations before and after super storm occurrences. These data are from space-based observations, so we will only be dealing with the more recent storms. We know of three cases in which a super storm, or events associated with a super storm, caused significant and long-lasting changes in trapped radiation populations, and one case where such effects were possible.

The best documented case of significant changes in the trapped particles occurred during the March 1991 storm. The CRRES satellite was in the slot region (near L = 2.5) at the time of a large shock associated SSC. Instruments on board CRRES measured a sharp jump in the local magnetic field, a large electric field pulse, and injections of protons (electrons) up to 75 (30) MeV [*Mullen et al.*, 1991; *Blake et al.*, 1992a, b; *Wygant et al.*, 1994]. The injected particles were stably trapped and persisted for many months, creating a new radiation hazard for satellites traversing the slot region.

An earlier report of significant changes in the trapped radiation environment was given by *Gussenhoven et al.* [1989], using dosimeter data from the Defense Meteorological Satellite Program (DMSP) during the February 1986 storm. The DMSP satellites are in low-altitude (840 km), high-inclination (99°) orbits. The dosimeter on DMSP indicated increased radiation levels (by an order of magnitude) at L = 2.5 after the February 1986 storm. As in March 1991, both high-energy protons (20–40 MeV) and electrons (>10 MeV) were measured. The increased dose rate lasted for several months.

A third case of significant changes in the high-energy inner magnetospheric particle environment was reported by *Spjeldvik and Fritz* [1981b] based on sensors on Explorer 45. Explorer 45 carried a heavy ion solid state detector telescope. Immediately following the super storm in August 1972, the telescope indicated enhancements of helium ions (1.16–3.15 MeV) by an order of magnitude near L = 2.5 R_E. These enhancements persisted for the remainder of the year.

Table 3. Largest Values of AE

Year	Day	Hour	Value, nT
	National Geophysical Data Center Data Set		
1958	42	0200–0300	2436
1958	189	1500–1600	2320
1960*	318	0900–1000	2172
1960*	318	1000–1100	2561
1968	46	1300–1400	2299
1970	67	1400–1500	2395
1972*	217	2200–2300	2065
1986*	39	1500–1600	2503
	Preliminary Data		
1991*	83	0400–0500	3014

*During super storms.

The final case that we are aware of in the literature comes from results from Explorer 14 (in late 1962) reported by *McIlwain* [1963]. These data show a second peak in 25–100 MeV protons near L = 2.5 R_E (similar to the one observed by CRRES). The peak had apparently faded by late 1963 [*McIlwain*, 1965]. McIlwain did not believe this peak was the result of the nuclear detonations in 1958 and 1960/1961 in the upper atmosphere and magnetosphere. We think it possible that this second peak was an enduring result of the November 1960 super storm. If that is true, the changes which occurred during that storm persisted for almost 2 years.

One might note that there are two super storms since 1960 that are not discussed above, the storm in July 1982 and the storm in March 1989. We have been unable to locate any data on the trapped radiation populations for the 1982 period, but there are DMSP data available during the March 1989 storm. *Mullen and Holeman* [1994] have shown that contamination of low-energy particle detectors on DMSP by >2–3 MeV electrons give a rough indication of time variations in this population. The time history of the contamination, as a function of L and intensity, have been constructed from 1984 to the present. The new radiation belts formed in 1986 and 1991 are clearly visible in the time history. However, in March 1989 the contamination data show particles penetrating deep into the magnetosphere, but these particles do not become trapped in the slot region. On the basis of the DMSP data the March 1989 storm does not appear to coincide with the creation of new, long-lived radiation populations in the slot region.

The question of why some storms cause major changes in the inner magnetospheric radiation populations while others do not is of great interest to the community and has been widely discussed. Clearly, it is not sufficient that the storm be a super storm. It has been suggested that the passage of two shocks in close proximity is required [*Mullen and Gussenhoven*, 1994], while others have considered a single large shock to be sufficient [*Li et al.*, 1993; *Hudson et al.*, this issue]. We would like to suggest the possibility that the spikes in AE, discussed above, may be an indicator of the intensity of the magnetospheric current system and/or the amount of distortion of the magnetosphere that accompanies the transport and energization of particles forming new belts in the slot region. Each of the four storms associated (or potentially associated) with the formation of new radiation belts in the slot region contains an AE spike, as discussed above. The occurrence of the AE spikes

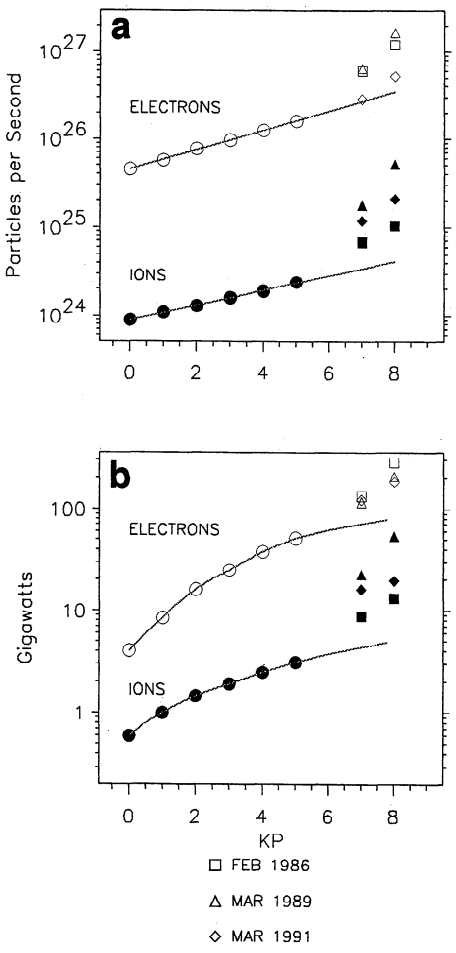

Figure 6. (a) The auroral number flux and (b) power input integrated over a single hemisphere as a function of *Kp*. Circles represent data from the *Hardy et al.* [1985, 1989] statistical maps of auroral precipitation; the other symbols represent maps made for highly disturbed and very highly disturbed periods during three super storms.

may be coincidental, but we consider it to be worth further investigation.

5. Auroral Particle Input During Super Storms

Total power input to near-Earth space from auroral particles during super storms can be extremely large. This is of major importance in assessing how the magnetospheric-ionospheric system can be reconfigured during the storms. Here we will examine in some detail the three most recent super storms for which we have auroral particle measurements. Since we know that auroral particle fluxes increase with increasing *Kp* (*ap*), we will use the *ap* index (so we can average) to determine the duration of high magnetic activity during the super storms. We identify for each super storm, the length of time the average *ap* exceeds two values: 108 and 220, which represent levels near the bottom end and the top end of the activity levels used to pick the largest storms from *ap* (see Table 1). We consider these two levels to be representative of "highly disturbed" and "very highly disturbed" periods. Below we examine the particle data and the power input during super storms.

The auroral particle detectors on the DMSP satellites measure precipitating ions and electrons from 30 eV to 30 keV. At least two detectors have been making measurements continuously since 1984, one traveling dawn to dusk, and one, prenoon to premidnight in local time. The data have been used to create maps of particle input to the auroral regions [*Hardy et al.*, 1985, 1989; *Brautigam et al.*, 1991]. One of the parameters used to order the data is *Kp*. So little data exist for $Kp \geq 6$ that integral maps were only made for *Kp* up through $Kp = 5+$. A catch-all bin for $Kp \geq 6-$ was created with the remaining data. See *Hardy et al.* [1985, 1989] for map construction details.

One output from the auroral maps is total integrated flux into the auroral region, called the hemispheric flux [*Brautigam et al.*, 1988, 1991]. From these flux maps, maps of the number flux and the total power input can be determined. Figure 6 shows the electron (open circles) and ion (closed circles) hemispheric number flux in particles per second (Figure 6a) and power input in gigawatts (Figure 6b) as a function of *Kp* taken from the *Hardy et al.* [1985, 1989] maps. It can easily be seen that the hemispheric number fluxes vary linearly over the *Kp* range, up to $Kp = 5$. The power, on the other hand, increases less as *Kp* gets higher, suggestive of a possible saturation effect. In both plots the data have been extrapolated out to a *Kp* of 9. The electron and ion contributions are plotted on the same scale, showing that the electron contribution is 1–2 orders of magnitude greater than that of the ions. The ion contribution to the total power input steadily decreases with increasing magnetic activity from 13% at $Kp = 0$ to 5.7% at $Kp = 5$.

Using the same technique that *Hardy et al.* [1985, 1989] used to make the original auroral maps, we created flux maps for the three super storms for which we have DMSP particle data: February 1986, March 1989, and March 1991. For each storm the maps were made by averaging all data taken in the two time periods when the *ap* averages were 108 and 220. These roughly correspond to average *Kp* values of 7 and 8, respectively. For these three super storms the averaging interval is 3.6, 4.4, and 4.0 days for $ap_{\text{ave}} = 108$, and 1.0, 1.5, and 0.5 days for $ap_{\text{ave}} = 220$.

The number flux and power input are given in Tables 4 and 5, and are shown by symbols in Figure 6. In all cases the electrons make the far greater contribution. The electron contributions increase by approximately a factor of 2 from the highly disturbed to the very highly disturbed period. The ion

Table 4. Hemispheric Auroral Number Flux

	$ap_{\text{ave}} = 108$		$ap_{\text{ave}} = 220$	
Storms	Electron	Ion	Electron	Ion
Feb. 1986	60.5	0.68	121	1.05
March 1989	64.5	1.79	168	5.15
March 1991	28.7	1.20	52.5	2.09

Flux is ($\times 10^{25}$ particles per second).

Table 5. Hemispheric Auroral Power Input

	$ap_{\text{ave}} = 108$		$ap_{\text{ave}} = 220$	
Storms	Electron	Ion	Electron	Ion
Feb. 1986	133	8.8	284	13.3
March 1989	117	22.5	209	54.0
March 1991	123	16.2	184	19.6

Input is in gigawatts.

increases are not as uniform, going from 20% to a factor of 3. Most importantly, Figure 6 shows that the super storm values are well above the extrapolated values. This is particularly true of the ion power input for the two March storms, where the ions contribute 21% (10%) of the total auroral power input in the very highly disturbed period of the March 1989 (1991) storm. The February 1986 storm, however, compares more closely to the power input from the *Hardy et al.* [1985, 1989], models, providing 6.2 and 4% of the power input for the highly disturbed and very highly disturbed storm periods, respectively. Thus it appears that during some super storms the auroral power input to the magnetosphere exceeds the apparent asymptotic saturation level. This is consistent with auroral particles seen at geosynchronous altitudes where the plasma beta can exceed 100 during the largest magnetic storm periods [*Mullen and Gussenhoven*, 1983]. (Note that the plasma beta is the ratio of particle pressure to magnetic field pressure. When the two are in balance, the plasma beta = 1. When the particles exceed the magnetic containment level, the value exceeds 1. This is consistent with the Kennel Petschek trapping limit [*Kennel and Petschek*, 1966] being exceeded for periods during large storms, and is not a steady state condition.)

Two comparisons help make the numbers associated with auroral particle input to one hemisphere during super storms more meaningful. First, the average power input to one hemisphere during the $ap_{ave} = 220$ period during the super storms in February 1986, March 1989, and March 1991 were 297, 263, and 204 gigawatts (GW), respectively. The average electrical power usage in the United States in 1988–1989 was 320 GW (Edison Electric Institute Statistical Yearbook). Second, the total precipitating particle energy calculated for these same storm periods was 2.5×10^{16}, 3.3×10^{16}, and 8.6×10^{15} J, respectively. These values are comparable to the work required to compress the magnetosphere to a standoff distance of 5 R_E.

6. Summary

We have shown that it is possible and reasonable to use numerical criteria applied to magnetic indices to select the largest magnetic storms based on magnitude and duration. The number of storms selected can be adjusted by varying these criteria. We selected the largest 2% of storms over the last 64 years (13 storms). These super storms were found to have occurred most often on the downslope from solar maximum. They were also found to occur most often near the equinoxes. Our examination of the morphology of the super storms points out the limitations of the data sets currently available. Consistently available solar wind data are critical for understanding the super storms. Our comparison of rearrangements of the trapped radiation populations with the super storms indicates that a relationship exists between the two. While not all super storms lead to rearrangements of trapped radiation populations, all known long-term changes appear to occur during super storms. It is possible that spikes in the *AE* data set may somehow be related to the new configurations as well.

Acknowledgments. The Editor thanks J. B. Blake and the other referee for their assistance in evaluating this paper.

References

Blake, J. B., M. S. Gussenhoven, E. G. Mullen, and R. W. Fillius, Identification of an unexpected space radiation hazard, *IEEE Trans. Nucl. Sci.*, *39*, 1761, 1992a.

Blake, J. B., W. A. Kolasinski, R. W. Fillius, and E. G. Mullen, Injection of electrons and protons with energies of tens of MeV into $L <$ 3 on 24 March 1991, *Geophys. Res. Lett.*, *19*, 821, 1992b.

Brautigam, D. H., M. S. Gussenhoven, and D. A. Hardy, The IMF B_z and solar wind speed dependence for precipitating ion hemispheric energy flux, *Adv. Space Res.*, *8*(9), 65, 1988.

Brautigam, D. H., M. S. Gussenhoven, and D. A. Hardy, A statistical study on the effects of IMF B_z and solar wind speed on auroral ion and electron precipitation, *J. Geophys. Res.*, *96*, 5525, 1991.

Cliver, E. W., and N. U. Crooker, A seasonal dependence for the geoeffectiveness of eruptive solar events, *Sol. Phys.*, *145*, 347, 1993.

Crooker, N. U., E. W. Cliver, and B. T. Tsurutani, The semiannual variation of great geomagnetic storms and the postshock Russell-McPherron effect preceding coronal mass ejecta, *Geophys. Res. Lett.*, *19*(5), 429, 1992.

Daly, E. J., F. van Leeuwen, H. D. R. Evans, and M. A. C. Perryman, Radiation-belt and transient solar-magnetospheric effects on Hipparcos radiation background, *IEEE Trans. Nucl. Sci.*, *441*, 2376, 1992.

Feynman, J., Solar cycle and long term changes in the solar wind, *Rev. Geophys.*, *21*, 338, 1983.

Frederickson, A. R., E. G. Holeman, and E. G. Mullen, Characteristics of spontaneous electrical discharging of various insulators in space radiations, *IEEE Trans. Nucl. Sci.*, *39*, 1773, 1992.

Ginet, G. P., W. J. Burke, and J. Albert, An analysis of electron energization seen in simulations of the March 24, 1991 SSC, *Eos Trans. AGU*, *75*(16), Spring Meet. Suppl., 305, 1994.

Gussenhoven, M. S., E. G. Mullen, and E. Holeman, Radiation belt dynamics during solar minimum, *IEEE Trans. Nucl. Sci.*, *36*, 2008, 1989.

Gussenhoven, M. S., E. G. Mullen, M. Sperry, K. J. Kerns, and J. B. Blake, The effect of the March 1991 storm on accumulated dose for selected satellite orbits: CRRES dose models, *IEEE Trans. Nucl. Sci.*, *39*, 1765, 1992.

Hardy, D. A., M. S. Gussenhoven, and E. Holeman, A statistical model of auroral electron precipitation, *J. Geophys. Res.*, *90*, 4229, 1985.

Hardy, D. A., M. S. Gussenhoven, and D. H. Brautigam, A statistical model of auroral ion precipitation, *J. Geophys. Res.*, *94*, 370, 1989.

Hudson, M. K., A. D. Kotelnikov, X. Li, I. Roth, M. Temerin, J. Wygant, J. B. Blake, and M. S. Gussenhoven, Simulation of proton radiation belt formation during the March 24, 1991 SSC, *Geophys. Res. Lett.*, *22*, 291, 1995.

Hudson, M. K., S. R. Elkington, A. D. Kotelnikov, J. G. Lyon, V. A. Marchenko, I. Roth, M. Temerin, J. B. Blake, M. S. Gussenhoven, and J. R. Wygant, Simulations of radiation belt formation during storm sudden commencements, *J. Geophys. Res.*, this issue.

Joselyn, J. A., and B. T. Tsurutani, Geomagnetic sudden impulses and storm sudden commencements: A note on terminology, *Eos Trans. AGU*, *71*(47), 1808, 1990.

Kennel, C. F., and H. E. Petschek, Limit on stably trapped particle fluxes, *J. Geophys. Res.*, *71*, 1, 1966.

Legrand, J. P., and P. A. Simon, Ten cycles of solar and geomagnetic activity, *Sol. Phys.*, *70*, 173, 1981.

Li, X., I. Roth, M. Temerin, J. R. Wygant, M. K. Hudson and J. B. Blake, Simulation of the prompt energization and transport of radiation belt particles during the March 24, 1991 SSC, *Geophys. Res. Lett.*, *20*, 2423, 1993.

Mayaud, P. N., *Derivation, Meaning and Use of Geomagnetic Indices*, *Geophys. Monogr. Ser.*, vol. 22, AGU, Washington, D. C., 1980.

McIlwain, C. E., The radiation belts, natural and artificial, *Science*, *142*, 355, 1963.

McIlwain, C. E., Redistribution of trapped protons during a magnetic storm, in *Space Research V*, p. 374, North-Holland, New York, 1965.

Mullen, E. G., and M. S. Gussenhoven, SCATHA Environmental Atlas, *Tech. Rep. AFGL-TR-83-0002*, Air Force Geophys. Lab., Hanscom Air Force Base, Mass., 1983.

Mullen, E. G., and M. S. Gussenhoven, Additional dynamics of the second proton belt formation during the March 1991 magnetic storm, *Eos Trans. AGU*, *75*(16), Spring Meet. Suppl., 304, 1994.

Mullen, E. G., and E. Holeman, MeV electrons as measured by the DMSP J4 detector, 1, Particle identification and verification, *Eos Trans. AGU*, *75*(44), Fall Meet. Suppl., 541, 1994.

Mullen, E. G., and K. P. Ray, Microelectronics effects as seen on CRRES, *Adv. Space Res.*, *14*(10), 797, 1994.

Mullen, E. G., M. S. Gussenhoven, K. Ray, and M. Violet, A double-

peaked inner radiation belt: Cause and effect as seen on CRRES, *IEEE Trans. Nucl. Sci.*, *38*, 1713, 1991.

Russell, C. T., and R. L. McPherron, Semiannual variation of geomagnetic activity, *J. Geophys. Res.*, *78*, 92, 1973.

Shea, M. A., D. F. Smart, J. H. Allen, and D. C. Wilkinson, Spacecraft problems in association with episodes of intense solar activity and related terrestrial phenomena during March 1991, *IEEE Trans. Nucl. Sci.*, *39*, 1755, 1992.

Spjeldvik, W. N., and T. A. Fritz, Energetic heavy ions with nuclear charge $Z \geq 4$ in the equatorial radiation belts of the Earth: Magnetic storms, *J. Geophys. Res.*, *86*, 2349, 1981a.

Spjeldvik, W. N., and T. A. Fritz, Observations of energetic helium ions in the Earth's radiation belts during a sequence of geomagnetic storms, *J. Geophys. Res.*, *86*, 2317, 1981b.

Violet, M. D., and A. R. Frederickson, Spacecraft anomalies on the CRRES satellite correlated with the environment and insulator samples, *IEEE Trans. Nucl. Sci.*, *40*, 1512, 1992.

Wygant, J. R., F. Mozer, M. Temerin, J. B. Blake, N. Maynard, H. Singer, and M. Smiddy, Large amplitude electric and magnetic field signatures in the inner magnetosphere during injection of 15 Mev electron drift echoes, *Geophys. Res. Lett.*, *21*, 1739, 1994.

J. T. Bell, M. S. Gussenhoven, and E. G. Mullen, Phillips Laboratory, Hanscom Air Force Base, MA 01731. (e-mail: bell@plh.af.mil)

(Received May 10, 1996; revised August 26, 1996;
accepted October 25, 1996.)